This is a repository copy of *Investigation of an actively controlled robot arm for vibration suppression in milling*.

White Rose Research Online URL for this paper:
https://eprints.whiterose.ac.uk/169351/

Version: Published Version

Proceedings Paper:
Ozsoy, M. orcid.org/0000-0002-3069-7377, Sims, N.D. orcid.org/0000-0002-6292-6736 and Ozturk, E. orcid.org/0000-0001-9982-2837 (2020) Investigation of an actively controlled robot arm for vibration suppression in milling. In: Papadrakakis, M., Fragiadakis, M. and Papadimitriou, C., (eds.) EURODYN 2020: Proceedings of the XI International Conference on Structural Dynamics. EURODYN 2020: XI International Conference on Structural Dynamics, 23-26 Nov 2020, Athens, Greece. European Association for Structural Dynamics (EASD) , pp. 4577-4589. ISBN 9786188507227

10.47964/1120.9372.19472

© 2020 The Authors. For re-use permissions, please contact the authors.

Reuse
Items deposited in White Rose Research Online are protected by copyright, with all rights reserved unless indicated otherwise. They may be downloaded and/or printed for private study, or other acts as permitted by national copyright laws. The publisher or other rights holders may allow further reproduction and re-use of the full text version. This is indicated by the licence information on the White Rose Research Online record for the item.

Takedown
If you consider content in White Rose Research Online to be in breach of UK law, please notify us by emailing eprints@whiterose.ac.uk including the URL of the record and the reason for the withdrawal request.

eprints@whiterose.ac.uk
https://eprints.whiterose.ac.uk/

Available online at www.easdprocedia.org
EASD Procedia EURODYN (2020) 4577-4589

EASD Procedia

EURODYN 2020
XI International Conference on Structural Dynamics
M. Papadrakakis, M. Fragiadakis, C. Papadimitriou (eds.)
Athens, Greece, 23–26 November 2020

INVESTIGATION OF AN ACTIVELY CONTROLLED ROBOT ARM FOR VIBRATION SUPPRESSION IN MILLING

Muhammet Ozsoy[1], Neil D. Sims[1], and Erdem Ozturk[2]

[1]Department of Mechanical Engineering, The University of Sheffield
Mappin Street Sheffield S1 3JD, UK
e-mail: mozsoy1@sheffield.ac.uk, n.sims@sheffield.ac.uk

[2] Advanced Manufacturing Research Center with Boeing, The University of Sheffield
Wallis Way, Rotherham, Sheffield S60 5TZ, UK
e-mail: e.ozturk@sheffield.ac.uk

Keywords: Robotic-assisted milling, Proof-mass actuator, Active chatter suppression, Stability, Flexible structures.

Abstract. *In recent years, the use of robotic systems to enhance the productivity of machining operations has received significant attention from the research and manufacturing communities. Robots have the potential to further improve productivity, for example by providing automated workpiece fixturing, or by providing a flexible and reconfigurable platform from which a variety of subtractive or additive manufacturing operations could be performed. One possible approach is the use of a robotic arm to provide additional fixturing or support of the workpiece during the machining operation. This can increase the stiffness of the workpiece system during machining, which can improve productivity by limiting the onset of undesirable vibrations such as chatter. Chatter is a form of self-excited vibration which leads to low surface quality of the workpiece, shortens the cutting tool life and increases the cutting forces. In this paper, an actively controlled robot arm is simulated in order to suppress the chatter, in an effort to further improve the chatter stability. During the milling operation, preload can be applied through the robot to support the flexible structure, however, the robot cannot suppress high-frequency forces. Since the stiffness and damping ratio of the large flexible structure vary during the operation due to material removal, active vibration control is performed. A proof-mass actuator is proposed that can provide 45 N force up to 2000 Hz with 2 mm stroke. The dynamic properties of the device are identified experimentally as part of a model of a robot fixture prototype. The robotic arm is modelled as a three degree of freedom system; this is combined with a simplified representation of the workpiece dynamics, and the proof-mass actuator, within a Matlab environment. The effect of active control on the chatter stability is evaluated, focussing initially on the use of direct velocity feedback as a control strategy. Estimated chatter stability predictions, along with time, frequency domain simulation results, show that the application of active control method in robotic-assisted machining can suppress the chatter vibrations during machining and hence increase productivity.*

ISSN:2311-9020 © 2020 The Authors. Published by EASD Procedia.
Peer-review under responsibility of the Organizing Committee of EURODYN 2020.
doi: 10.47964/1120.9372.19472

1 INTRODUCTION

Thin-walled structures such as jet engine parts and aerospace fuselage components are common in the aeronautical industry. However, large flexibility of these components leads to excessive vibrations which are called chatter vibration during machining. Chatter is a form of self-excited vibration which leads to low surface quality of the workpiece, shortens the cutting tool life and increases the cutting forces. Milling stability theory [1] can be used to improve the chatter stability by selection of the process parameters which are cutting speed, feed rate and depth of cut. Also, in order to increase the productivity of the process, dynamic stiffness and damping ratio of the workpiece can be improved. There are many techniques with fixed supports [2] and mobile supports [3] to avoid chatter but an interesting current approach is to use robotic systems as part of the machining system. Robots can be used to directly machine components, yet they tend to exhibit very low stiffness which exacerbates excessive vibration. Recently, considerable literature has grown up around the theme of robotic assisted machining. Robots can be used to improve the fixturing or support of the workpiece during machining. The method is called robotic assisted milling when a robot supports a workpiece from the opposite surface to the milling process.

For instance, Ozturk et. al. [4] presented a new concept called robotic assisted milling of thin-walled structures. The authors used two types of end effectors to support the workpiece from the back surface. Experimental results showed that the surface roughness decreased considerably by using moving support. During the milling, robot and the cutting tool moved synchronously. As it is mentioned in the paper, the process was monitored not controlled. The authors did not take account of stiffness change during machining. As the workpiece's stiffness changes due to the material removal, the supporting force needs to be adjusted to achieve better dynamic response improvement.

Fei et al. [5] presented a moving damper to increase the stability of the process. Stability of the process increased substantially. Nonetheless, since the moving damper is fixed to the machine itself, it can be used for only a particular workpiece unless the moving damper design is changed. The authors also investigated the deformation model for moving fixture [6]. Surface quality and machining errors are improved. Esfandi and Tsao [7] suggested using an industrial robotic manipulator to avoid machining vibrations for turning process of the thin walled cylindrical structures. The results encouraged the use of manipulator which provides higher cutting stiffness. Nevertheless, the robot sometimes influences negatively the stability of the machining process given that the robotic arm itself is not rigid.

Some researchers have also studied the effect of the supporting preload force. Bo et al. [8] investigated the influence of supporting force of moving support on machining stability during mirror milling operation of the thin-walled structure. Supporting force influences not only machining stability but also the dynamic behaviour of the workpiece.

In this paper, an actively controlled robot arm which is modelled as a three degree of freedom system, is simulated for milling process in time and frequency domain. The aims are to improve chatter stability, select the most effective actuator assembly point, and compare the effect of the contact type between robot and workpiece. In section 2, contact parameter identification using the receptance coupling formula is presented. In section 3, an inertial actuator which can provide active control for robotic assisted milling is introduced. The effect of the active control on the chatter stability improvement is simulated and evaluated, focussing on the direct velocity feedback (DVF) as a control strategy. In the last section, the stability lobe diagram is estimated for the process.

2 IDENTIFICATION OF CONTACT PARAMETERS

The proposed robot and machine tool configuration is shown schematically in Figure 2.1. Here, a flexible robot is pushed against a flexible workpiece via a soft contact interface whose dynamics must be identified. The machining stability can be improved by using an active vibration control device on the end effector. During the milling operation, preload will be applied through the STAUBLI TX90 robot to stiffen the flexible workpiece. It should be noted that for the purposes of this proof-of-concept experiment, a nominal 'thin walled workpiece', is replaced by a solid workpiece block that is mounted on a flexure. The contact parameters which are stiffness and damping ratio, between the end-effector that is hard rubber, and the flexure are identified by receptance coupling formula [9]. Parameters are identified when 240 N support force is applied to the flexure.

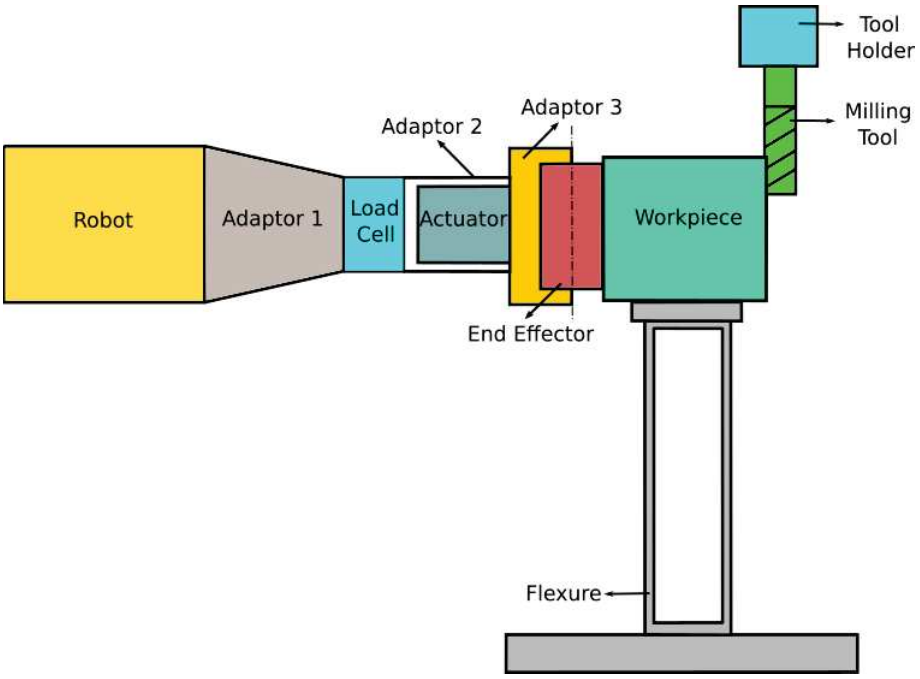

Figure 2.1: Actively Controlled Robot Arm for Milling

The workpiece and robot are modelled as single and three degree of freedom system, respectively. The combined system's frequency response function (FRF) is calculated as;

$$FRF_{combined} = FRF_{part} - FRF_{part}(FRF_{part} + FRF_{robot} + \frac{1}{K'})FRF_{part} \tag{1}$$

$$K' = k + iwc \tag{2}$$

where $FRF_{combined}$, FRF_{part}, FRF_{robot}, k, c and w are the combined FRF, workpiece FRF, robot FRF, contact stiffness, damping and the frequency, respectively.

As a first step, flexure and robot were tested using a modal hammer and accelerometer. The flexure FRF was measured at its midpoint. Since the robot's stiffness varies due to the configuration, the robot was tested on the end-effector while the robot was not touching the flexure but very close to the measurement point. Then, the experiments were repeated with

hard rubber supporting the workpiece at the middle point of the flexure. The flexure flexibility is improved 61% by utilizing preload through the robot as seen in Figure 2.2. Seeing that the experimental contact is flexible, the coupled system's natural frequency is changed from 380 Hz to 399 Hz. The contact stiffness and damping are identified for flexible contact as 4.5e5 N/m and 35.5 Ns/m, respectively.

Also, the combined FRF is estimated for rigid contact. If the contact was assumed as rigid contact, which can be provided with a metal castor end-effector presented by Barrios et. al. [10] by using a different robot, natural frequencies would have been shifted close to robot's natural frequencies which are 32, 76 and 136 Hz.

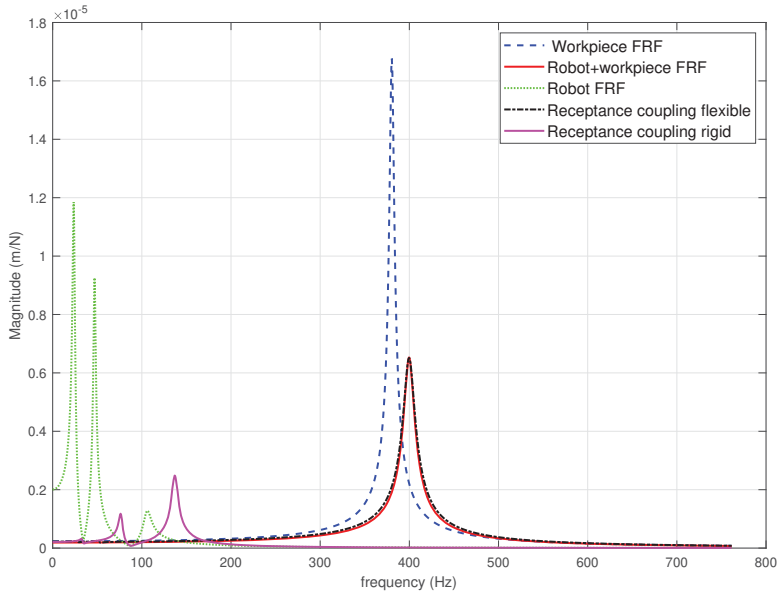

Figure 2.2: Frequency Response Functions and Receptance Coupling Model

3 ACTIVE CONTROL AND SIMULATION RESULTS

Active control is simulated for robotic assisted milling by using an actuator as shown in Figure 2.1. The direct velocity feedback (DVF) control system is selected as it is a model free control method and easy to apply. Once it is implemented, only the gain needs to be adjusted. An inertial actuator is chosen as this approach is easily deployed on the robot's end effector.

3.1 Inertial Actuator

The inertial actuator seen in Figure 3.1 can be represented by a vibrating mass m_p with a damper c_p and spring k_p. The mass is excited by a electromagnetic force f_a according to the voltage input V_{in}. The transfer function between the mass displacement x and the voltage input V_{in} can be written as,

$$\frac{x(s)}{V_{in}(s)} = \frac{G_1 G_2}{ms^2 + cs + k} \tag{3}$$

where G_1 is the electromagnetic gain and G_2 is the power amplifier gain [11].

The transfer function between the reaction force f_a and the voltage input V_{in} can be written as,

$$\frac{f_a(s)}{V_{in}(s)} = \frac{-G_1 G_2 m s^2}{ms^2 + cs + k} = g_a \frac{s^2}{s^2 + 2\zeta\omega_p s + \omega_p^2} \tag{4}$$

where ω_p is the natural frequency, ζ is the damping ratio of the actuator and g_a is the actuator gain [11].

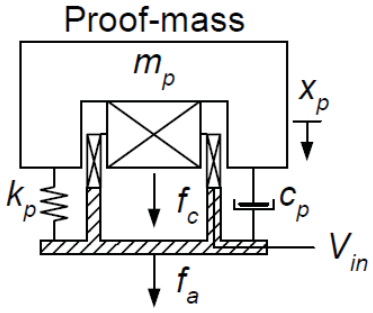

Figure 3.1: Proof-Mass Actuator [12]

An inertial actuator which is a model of Micromega Dynamics, is used to perform the simulations. This actuator has a mode at 8.4 Hz and is capable of applying up to 45 N supporting force up to 2000 Hz. Its transfer function [13] can be written as:

$$\frac{f_a(s)}{V_{in}(s)} = 5\frac{s^2}{s^2 + 15.834s + 2785.6} \tag{5}$$

3.2 Case Studies

In this section, 4 cases which show the effect of the actuator, actuator assembly point, and effect of the contact parameters, are presented. Time domain solutions are solved by ODE 45 function within a Matlab environment. This function implements a Runge-Kutta method with a variable time step for the time domain solution. Robot and workpiece are modelled as a three and single degree of freedom, respectively. Model parameters and cases can be seen in Table 3.1 and Table 3.2.

Table 3.1: Model Parameters

Parameters	Value (kg)	Parameters	Value (N/m)	Parameters	Value (Ns/m)
M_1	32.8	K_1	7.3e5	C_1	573
M_2	21.6	K_2	1.88e6	C_2	368
M_3	21.4	K_3	9.47e6	C_3	1210
M_4	0.748	K_4	4.5e5	C_4	35.5
M_a	1	K_5	4.27e6	C_5	25
		K_a	2785.6	C_a	15.83

Table 3.2: Cases

Case Number	Explanation
Case 1	Preloaded case, without actuator
Case 2	Actuator on the end-effector, flexible contact
Case 3	Actuator on the end-effector, rigid contact
Case 4	Actuator on the workpiece, flexible contact

The first case is uncontrolled and has a flexible contact. Three degree of freedom robot supports the workpiece. Vibration on the workpiece is suppressed by applying preload through the robot. Its spring-mass model can be seen in Figure 3.2.

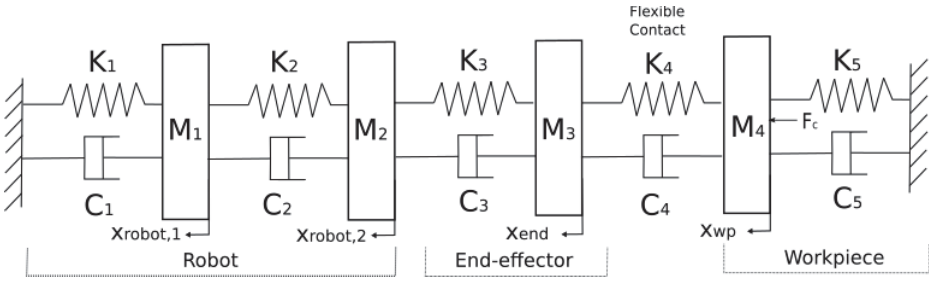

Figure 3.2: Flexible Contact Without Actuator

The natural frequency of the workpiece is shifted from 380 Hz to 399 Hz in this configuration. The model natural frequency is calculated by Cramer's rule [14]. The amplitude of the workpiece is reduced by around 61%. This scenario matches the results already presented in Figure 2.2.

Case 2 is with the actuator mounted on the end-effector seen in Figure 3.3. So as to carry out the direct velocity feedback (DVF) control method, vibration of the end-effector is differentiated to velocity and the velocity is multiplied with feedback gain to drive the actuator.

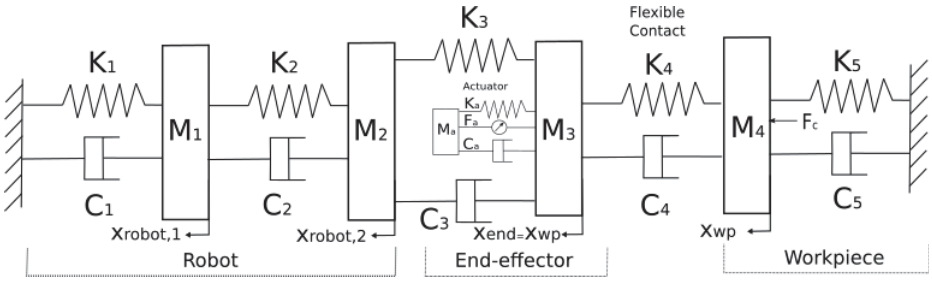

Figure 3.3: Actuator on the End-effector with Flexible Contact

The simulated FRF for this case is shown in Figure 3.4. The input force is implemented on the end-effector and workpiece while output is measured on workpiece for both simulations. Direct FRF (red dashed line) for the workpiece has only one mode at 399 Hz yet the cross FRF (blue solid line) has two modes at 19 Hz and 54 Hz. In practice when the optimum gain limit is exceeded, the system becomes unstable due to actuator nonlinearities such as force and stroke

saturation. So, the optimum actuator gains were determined via simulations and the best case scenario is presented in Figure 3.5. In the simulations, a sinusoidal excitation force of 100 N at 399 Hz, was applied to the workpiece to approximately represent the forces due to the milling operation. Figure 3.5 shows the simulated workpiece response under these conditions. It can be seen that the actuator cannot provide enough force to suppress the vibration on the workpiece since the vibration on the end-effector is too small due to the flexible contact. Consequently, the actuator is ineffective and the workpiece vibrations are not suppressed.

Nevertheless, if the system is excited with 100 N at 19 Hz, vibration on the workpiece is suppressed by 23% shown in Figure 3.5b. Vibration on the workpiece is decreased up to feedback gain g=800. Gain greater than 800 makes the system unstable due to the actuator nonlinearity.

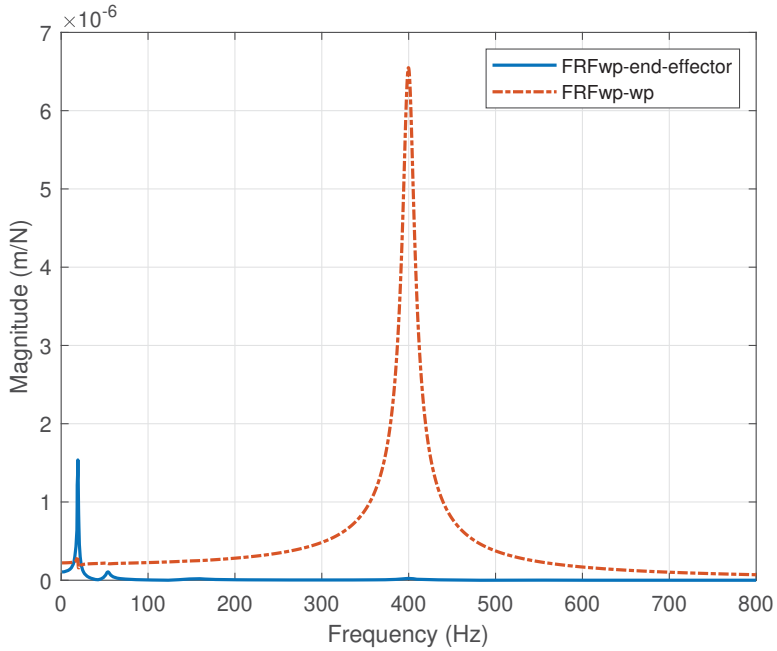

Figure 3.4: Frequency Domain Model for Case 2

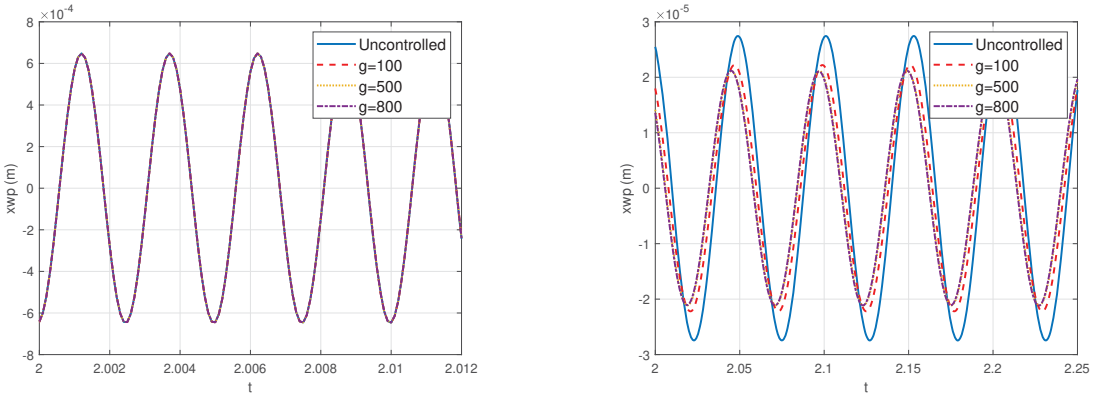

(a) Excitation Force at 399 Hz

(b) Excitation Force at 19 Hz

Figure 3.5: Workpiece Vibration for Case 2

Case 3 is with the actuator on the end-effector with rigid contact (metal castor) as shown in Figure 3.6. Since the vibration on the end-effector is equal to workpiece's vibration, the actuator can provide the vibration suppression on the workpiece. Rigid contact decreases the natural frequencies to 34, 65, 160 Hz. All three modes are damped by active control.

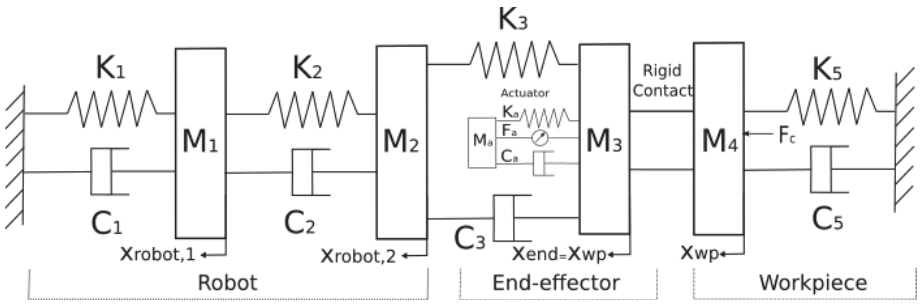

Figure 3.6: Actuator on the End-effector with Rigid Contact

To excite the system a sinusoidal force which is 50 N at 65 Hz is applied. 65 Hz is the most flexible frequency for the workpiece. Actuator force varies from 13 N to 45 N for the gains: 100 (dashed red line), 500 (dotted yellow line), 1000 (dash-dot purple line), 2500 (solid green line) and blue solid line is for the uncontrolled system shown in Figure 3.7. Workpiece vibration is suppressed around 90% for the case 3. Since the maximum produced force by the actuator is 45 N, gain can be increased up to 2500 for this excitation force value. If the gain is selected greater than 2500, the system will be unstable owing to the force saturation.

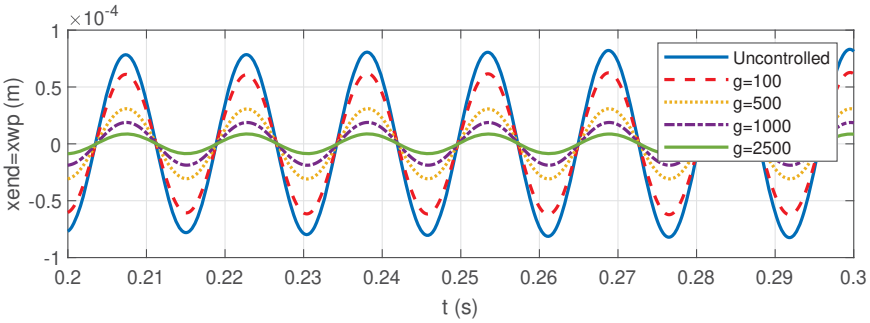

Figure 3.7: Time Domain Model with Rigid Contact

Case 4 with actuator on the workpiece can be seen in Figure 3.8. The contact between the end-effector and the workpiece is flexible. In this case, the support is fixed support since the actuator is assembled directly to the workpiece. 50 N at 399 Hz sinusoidal excitation force is implemented. Optimum gain is determined as 5000, yet the gain only can be increased to 150 owing to the actuator force limitation. Time domain result is shown in Figure 3.9. Actuator force varies from 20 N to 45 N for the gains 10 (dashed red line), 50 (dotted yellow line), 100 (dash-dot purple line), 150 (solid green line). Vibration on the workpiece is suppressed around 90%. If the gain was increased up to 5000 without actuator force limitation, vibration on the workpiece could have been suppressed around 99%.

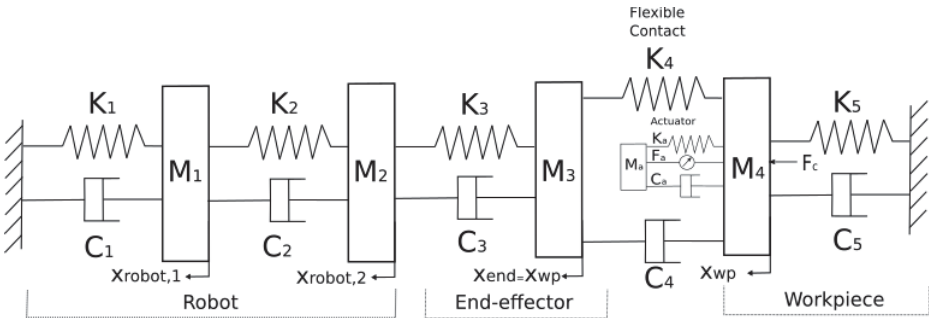

Figure 3.8: Actuator on the Workpiece

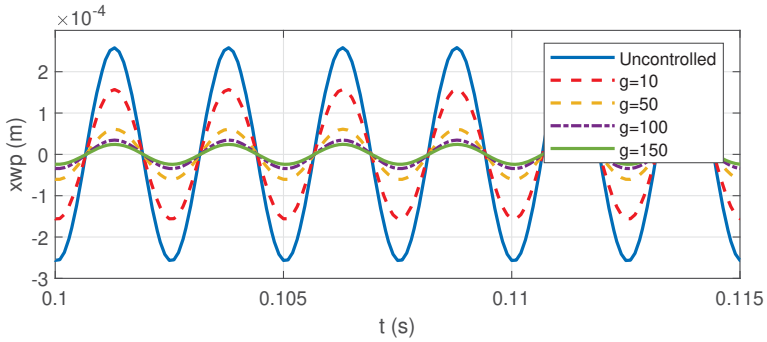

Figure 3.9: Time Domain With Actuator on the Workpiece

All the cases are compared in regards of workpiece vibration whilst the robot applies the preload to the midpoint of the flexure. The effect of preload point can affect the results slightly, which is given in the next section.

3.3 The Effect of Robot Position

The robot applied the preload to the midpoint of the flexure in the previous section. The flexibility of the flexure is improved 61%. However, if the robot applies the preload to the edge point of the flexure, the flexibility is improved 51%. Case 4 results are compared for both robot's preload position and it is presented in the Figure 3.10. The DVF control method is applied with the same gains (10, 50, 100, 150) to the case 4 for both robot's position. In terms of controlled vibration results, there is no significant difference.

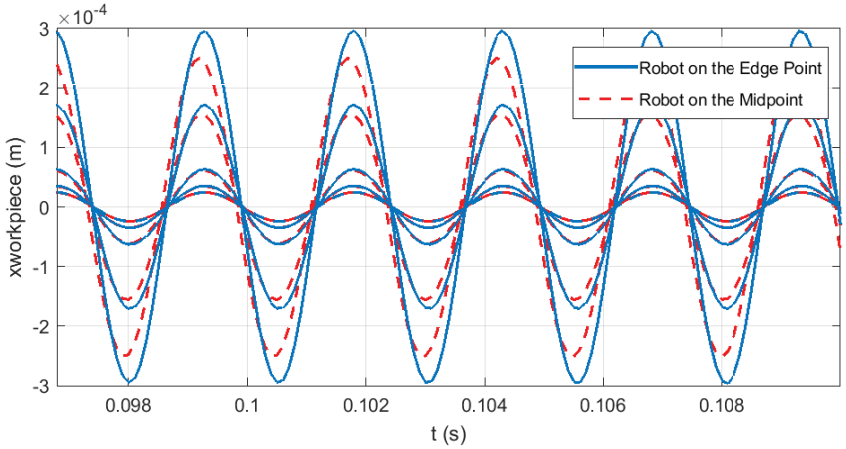

Figure 3.10: Comparison of Robot's Position Effect on Vibration Result

All cases are evaluated regarding vibration of the workpiece. By using active control through the robot, the dynamic response of the structure can be improved significantly. Contact parameters and the actuator assembly point are very critical in order to get a well damped and stable system. Selection of the end-effector and the actuator assembly point must be taken into consideration for further applications. From a machining context the implications of this vibration suppression can be considered from the perspective of the chatter stability. This is considered in the next section.

4 STABILITY LOBE DIAGRAM

Selection of proper axial depth of cut and spindle speed is important to avoid chatter vibrations [1]. Stability lobe diagram is often used to select optimal parameters so as to improve productivity. The stability lobe diagram is estimated for the robot configurations described in Section 3 in order to demonstrate the performance improvement that can be obtained from a manufacturing context.

The stability lobe diagrams were obtained using Budak and Altintas's method [15]. Details of this approach are outside the context of the current contribution, but the theory and method is widely reported elsewhere [1,15]. Down milling was a assumed, with a 20 mm diameter 4 tooth tool and a radial immersion of 3 mm. The workpiece was assumed to have a cutting stiffness of Ks=796e6 N/m2, Kt=768e6 N/m2, corresponding to Al-7075-T6 material. With reference to Figure 4.1, five scenarios are shown:

- Flexible workpiece without active control and preload (blue solid line)
- Case 1: With preload which is implemented through the robot arm (red dashed line)
- Case 3: With the actively controlled robot arm by the inertial actuator on the end-effector, rigid contact (for g=150 dotted green line, for g=2500 purple dash-dot line)
- Case 4: With the actively controlled robot arm by the inertial actuator on the workpiece, flexible contact (for g=150 black solid line)

SLD is not developed for case 2 since the FRF was no improved in this scenario.

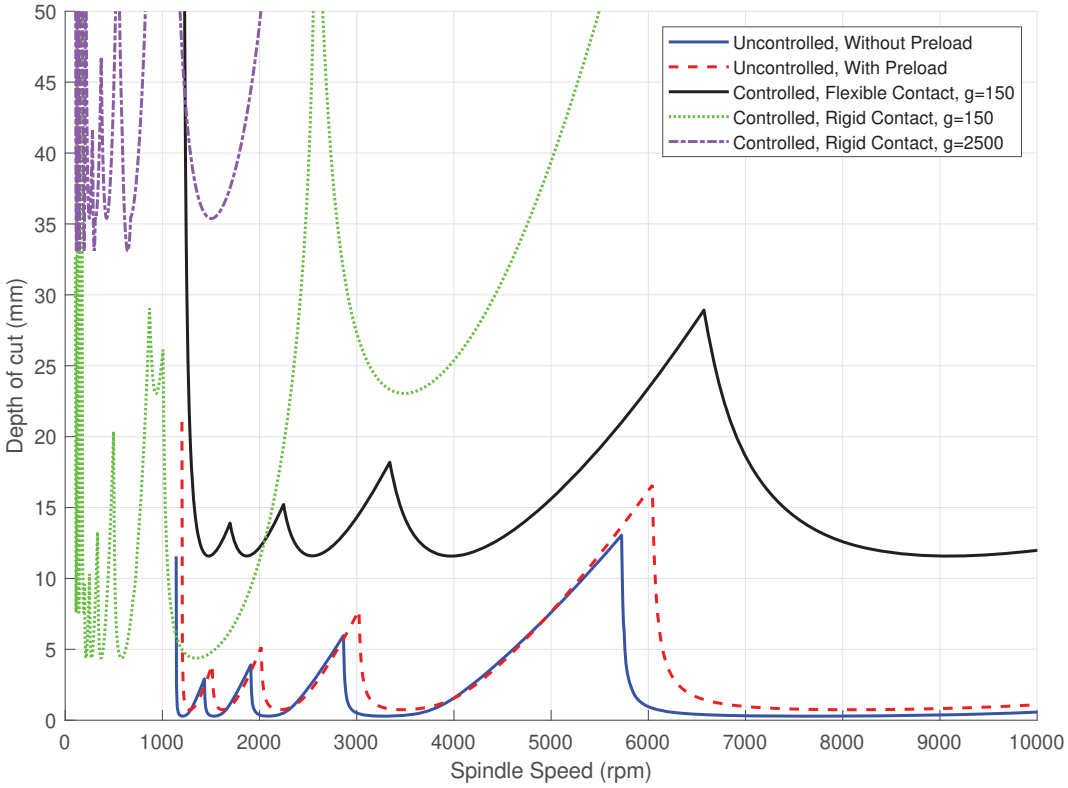

Figure 4.1: Stability Lobe Diagram

Comparison of the limiting (min) depth of cut for each cases can be seen in Table 4.1.

Table 4.1: Comparison of the Limiting Depth of Cut b_{lim}

Cases	blim (mm)
Uncontrolled, Without Preload	0.29
Case 1, Uncontrolled, With Preload (240 N)	0.74
Case 3, Controlled, Actuator on the End-Effector, Rigid Contact, g=150	4.38
Case 3, Controlled, Actuator on the End-Effector, Rigid Contact, g=2500	33.09
Case 4, Controlled, Actuator on the Workpiece, g=150	11.58

As seen in Figure 4.1 and Table 4.1, the depth of cut is increased around 2.5 times with preload through the robot arm. To achieve greater depth of cut, active vibration control is applied. The greatest depth of cut is achieved when the actuator is assembled on the end-effector with rigid contact, gain=2500. However, when the actuator is mounted directly onto the workpiece, the depth of cut is improved more than when the actuator is mounted on the end-effector.

5 CONCLUSIONS

The purpose of the current study is to determine the dynamic response improvement in milling operation by using an actively controlled robot arm. The concept is evaluated in terms

of the contact type between the robot, workpiece, and actuator. Direct velocity feedback (DVF) control method is performed in order to improve the dynamic response. It is concluded that the actively controlled robot arm can improve the productivity of the milling process by decreasing the vibration on the workpiece.

In the conducted simulations, workpiece vibration is damped around 61% by applying preload through the robot to the midpoint of the flexure. An inertial actuator is mounted on the end-effector and the workpiece for different cases to compare the effect of the actuator assembly point on the dynamic response. An actuator on the end-effector with flexible contact cannot improve the dynamic response of the workpiece except at low frequencies. However, when the actuator is assembled on the end-effector with rigid contact, the vibration on the workpiece is significantly decreased to around 90%. If the actuator is mounted directly onto the workpiece, rather than via the robot, then the workpiece vibration decreases by around 90%. Similar performance improvements can be observed in the so-called stability lobe diagram for a machining scenario. To summarise, the work has proved the concept of using a robotically assisted active vibration control system, for the machining of flexible workpieces. It has been shown via simulations that improved machining stability can be achieved even when accounting for the flexibility of the robot and the workpiece to robot contact.

As future work, all the simulations will be validated by experimental study. Direct velocity feedback control method will be compared with more sophisticated control methods such as PID, LQG, LQR and H_∞. Finally, different end-effectors can be designed to compare the contact parameter effect on the chatter stability.

REFERENCES

[1] Y. Altintas, *Manufacturing automation: metal cutting mechanics, machine tool vibrations, and CNC design*. Cambridge university press, 2012.

[2] K. Kolluru, D. Axinte, and A. Becker, "A solution for minimising vibrations in milling of thin walled casings by applying dampers to workpiece surface," *CIRP Annals-Manufacturing Technology*, vol. 62, no. 1, pp. 415–418, 2013.

[3] C. Sun, P. L. Kengne, A. Barrios, S. Mata, and E. Ozturk, "Form error prediction in robotic assisted milling," in *Procedia CIRP*, vol. 82. Elsevier, 2019, pp. 491–496.

[4] E. Ozturk, A. Barrios, C. Sun, S. Rajabi, and J. Munoa, "Robotic assisted milling for increased productivity," *CIRP Annals*, 2018.

[5] J. Fei, B. Lin, S. Yan, M. Ding, J. Xiao, J. Zhang, X. Zhang, C. Ji, and T. Sui, "Chatter mitigation using moving damper," *Journal of Sound and Vibration*, vol. 410, pp. 49–63, 2017.

[6] J. Fei, B. Lin, J. Xiao, M. Ding, S. Yan, X. Zhang, and J. Zhang, "Investigation of moving fixture on deformation suppression during milling process of thin-walled structures," *Journal of Manufacturing Processes*, vol. 32, pp. 403–411, 2018.

[7] N. Esfandi and T.-C. Tsao, "Robot assisted machining of thin-walled structures," *IFAC-PapersOnLine*, vol. 50, no. 1, pp. 14 594–14 599, 2017.

[8] Q. Bo, H. Liu, M. Lian, Y. Wang, and K. Liu, "The influence of supporting force on machining stability during mirror milling of thin-walled parts," *The International Journal of Advanced Manufacturing Technology*, pp. 1–13, 2018.

[9] T. L. Schmitz and K. S. Smith, *Machining dynamics*. Springer, 2014.

[10] A. Barrios, S. Mata, A. Fernandez, J. Munoa, C. Sun, and E. Ozturk, "Frequency response prediction for robot assisted machining," *MM Science Journal*, vol. 2019, no. 04, pp. 3099–3106, 2019.

[11] A. Preumont, *Vibration control of active structures*. Springer, 1997, vol. 2.

[12] S. Huyanan and N. D. Sims, "Vibration control strategies for proof-mass actuators," *Journal of Vibration and Control*, vol. 13, no. 12, pp. 1785–1806, 2007.

[13] Operational and M. Manual, *Micromega Dynamics*. Belgium, 2019.

[14] S. S. Rao, "Mechanical vibrations fifth edition in si units," 2012.

[15] Y. Altintaş and E. Budak, "Analytical prediction of stability lobes in milling," *CIRP Annals-Manufacturing Technology*, vol. 44, no. 1, pp. 357–362, 1995.